

## Stable and degradable microgel linked with cystine for storing and environmentally triggered release of drugs

Marcin Mackiewicz<sup>1</sup>, Klaudia Kaniewska<sup>1</sup>, Jan Romanski<sup>1</sup>, Ewa Augustin<sup>2</sup>, Zbigniew Stojek<sup>1</sup>,

Marcin Karbarz<sup>1,\*</sup>

<sup>1</sup>Faculty of Chemistry, University of Warsaw, Pasteura 1, PL 02-093 Warsaw, Poland

<sup>2</sup>Department of Pharmaceutical Technology and Biochemistry, Gdansk University of Technology, Narutowicza 11/12, 80-233 Gdansk, Poland

\*Corresponding author

E-mails: [karbarz@chem.uw.edu.pl](mailto:karbarz@chem.uw.edu.pl), [stojek@chem.uw.edu.pl](mailto:stojek@chem.uw.edu.pl)

## Abstract

Environmentally sensitive, degradable microgels based on poly(*N*-isopropylacrylamide) (pNIPA) cross-linked with diacryloyl derivative of cystine (BISS) were synthesized by applying the surfactant-free emulsion polymerization. pNIPA contributed the sensitivity to temperature to the microgels and the cross-linker made them degradable and sensitive to pH. Morphology of the microgels was investigated by using the scanning- and transmission electron microscopies (SEM and TEM). The gels formed spherical particles with a narrow size distribution. The influence of temperature, pH and ionic strength on the swelling behavior and the stability of new microgels with various content of BISS (0, 1 and 3%) were investigated by dynamic light scattering (DLS). It was found that the microgels with 3% content of the amino acid were highly stable in wide ranges of investigated temperature, pH and ionic strength, including the physiological conditions (pH = 7.4, IS = 0.15 M, 37 °C). The reduction-induced degradation of these microgels by 0.01 M solution of dithiothreitol (DTT) or glutathione (GSH) were studied by means of SEM and TEM; the obtained micrographs showed the destruction of spherical microgel particles. The microgels containing 3% of BISS could be loaded with doxorubicin (DOX) by employing the electrostatic interactions between the DOX amine group and the ionized carboxyl group from BISS. A significant increase in cumulative release of DOX was observed after changing pH from that characteristic to blood (~7.4) to that existing in affected cells (~5.0) and in the presence of GSH ( $C_{\text{GSH}} \sim 10$  mM). The cytotoxicity tests proved that the obtained microgels are interesting as useful carriers in directed drug delivery systems.

**Keywords:** microgel, degradation, cystine, disulfide bridges, *N*-isopropylacrylamide, glutathione, drug delivery



## 1. Introduction

Microgels are chemically cross-linked polymers, with a network structure, that are colloidal in size and swollen in a suitable solvent. The networks containing water are called hydrogels. They, similarly to bulk gels, possess high water content, are usually biocompatible and their interior network is responsible for storing the mechanical energy and providing the desired mechanical properties. The relatively small molecules can diffuse almost freely in the swollen gels. However, larger individuals can be immobilized in their internal structure. The gels are environmentally sensitive and are able to switch their properties in response to an external stimulus. They can exist in two different states: swollen and collapsed (shrunken), and the transition from one state to another is called the volume phase transition. The reversible transition occurs as a response to changes in environmental conditions (such as temperature, pH, ionic strength, presence of specific ions, pressure, solvent composition and electromagnetic radiation).<sup>1-4</sup> In contrast to bulk hydrogels, microgels are injectable, have a very high surface area to volume ratio and respond much faster to environmental stimuli. Microgels have attracted interest as the materials for sensors,<sup>5,6</sup> catalysts,<sup>7</sup> optical devices and vehicles in drug delivery systems.<sup>8-11</sup>

Particularly attractive are the microgels based on thermoresponsive polymers because of their potential use in biomedical applications.<sup>12</sup> Among them, the microgels based on *N*-isopropylacrylamide (NIPA) are of increased interest. The cross-linked poly(*N*-isopropylacrylamide) (pNIPA) hydrogels are known to exhibit a drastic volume phase transition (they turn into the collapsed state) at a temperature above 32 °C. At any temperature lower than 32 °C these gels are swollen. There used to be some limitations in using this polymer as a vehicle in drug delivery system: its cytotoxicity and non-degradable nature. However, recently it has been shown that poly(*N*-isopropylacrylamide) is effectively noncytotoxic at concentrations realistic to many medical applications.<sup>13-15</sup> Non-degradability

of these materials is a result of the presence of a non-cleavable cross-linker. To discard this inconvenience the cross-linkers that contain disulfide bonds can be used. A few examples of microgels that incorporated the degradability, usually by using commercially available *N,N'*-bis(acryoyl)cystamine (BAC), are presented in literature.<sup>16-19</sup> An interesting substitute for bis(acryoyl)cystamine can be derived from natural amino acid cystine (*N,N'*-bisacryloylcystine, BISS). To our best knowledge there are no examples of using this cross-linker in the microgel systems. BISS was used only in polymer systems<sup>20,21</sup> to provide disulfide links in the main chain. We used it as the co-crosslinker for further modification of polymeric gels based on *N*-isopropylacrylamide.<sup>22</sup>

The cleavage reaction of the disulfide bonds present in cross-linkers in microgels can lead to the gel degradation and to release of loaded compounds.<sup>18</sup> A variety of disulfide-bond reductants can be used. In biochemistry, thiols such as dithiothreitol (DTT) and mercaptoethanol serve as the reductants. DTT is an unusually strong reducing agent, because once oxidized, it forms a stable six-membered ring with an internal disulfide bond. DTT is frequently used to reduce the disulfide bonds of proteins and to prevent the disulfide-bond formation between cysteine molecules in proteins. From biomaterials point of view it is very important that disulfide bonds can be cut in response to physiological relevant reducing conditions. Glutathione tripeptide (GSH) is the most abundant low-molecular-weight biological thiol and GSH with its oxidized form (GSSG) form the major redox couple in animal cells.<sup>23</sup> It is known that there is a significant difference in the redox potentials of this couple in the extracellular and intracellular environments.<sup>24-27</sup> The reduction-sensitive degradable microgels can be degraded and can release drugs at high reducing conditions in the cytoplasm (0.5–10 mM) in which the concentration of GSH is up to 1000 fold higher compared to the extracellular fluids (about 2–20  $\mu$ M).<sup>28</sup> Furthermore, it has also been found that there exists about 4-fold higher concentration of GSH in tumor tissues than in the normal



tissues. Tumor tissues are highly reducing and hypoxic compared with normal tissues. GSH concentration is also dependent on the cell types, e.g. reaches ca. 5 mM level in blood cells (as we mentioned before) and 30 mM in liver cells.<sup>29-33</sup> Therefore, the potential of disulfide cross-linked reduction-sensitive systems are attractive for anticancer drug delivery.

In the present study, we obtained new microgels based on *N*-isopropylacrylamide cross-linked with bisacryloyl derivative of cystine using the aqueous precipitation polymerization. The derivative of cystine makes the microgels degradable similarly to commercially available cross-linker *N,N'*-bis(acryloyl)cystamine; however, it has two advantages: 1) it is significantly better soluble in aqueous media and 2) allows simultaneous introduction of carboxylic groups into the polymeric network. The presence of carboxylic groups makes the gels sensitive to pH, improves their stability vs. ionic strength and allows further chemical modification of the chains. In this work we focused our attention on the influence of temperature, pH and ionic strength on swelling behaviour and stability of the microgels synthesized with various amount of this cross-linker. The influence of the presence of the reducing agents on microgel degradation and usefulness of the gels as drug carriers were also investigated.

## 2. Experimental

### 2.1. Chemicals

*N*-isopropylacrylamide (NIPA, 97%), potassium persulfate (KPS, 99.99%), DL-dithiothreitol (DTT, 98%), L-glutathione reduced (GSH, 98%), 5,5'-Dithiobis(2-nitrobenzoic acid) (DTNB, 98%) and acryloyl chloride (96%) were purchased from Aldrich. Sodium hydroxide (NaOH, 99%), hydrochloric acid (HCl, 35-38%) and L-cystine (98,5%) were purchased from POCh.

All chemicals were used as provided by the manufacturers except for NIPA, which before experiments was recrystallized twice from benzene/heksane mixture (9:1). All solutions were prepared using high purity water obtained from a Hydrolab/HLP purification system (water conductivity: 0.056  $\mu\text{S cm}^{-1}$ ).

### 2.2. Synthesis of disulfide cross-linker, *N,N'*-bisacryloylcystine (BISS)

The disulfide cross-linker was synthesized according to the modified method described previously.<sup>34</sup> To a stirred solution of sodium hydroxide (2g, 50 mmols) and cystine (2.70 g, 11.2 mmols) in methanol (70 ml), acryloyl chloride (2.20 ml, 27.2 mmols) was added dropwise at 0°C. The solution was stirred at room temperature and after 4h the reaction mixture was filtered through a celite pad. The filtrate was added dropwise into intensively stirred cold diethyl ether. The obtained suspended solid was isolated by filtration, washed with diethyl ether and dried under high vacuum at 30-45 °C. The percentage of disodium salt of *N,N'*-bisacryloylcystine in the powder was determined to be 60 to 70 % using the combustion analysis based on sulphur content. Then the disodium salt of *N,N'*-bisacryloylcystine was converted into carboxylic acid and separated from the inorganic salt (NaCl). For this purpose the aqueous solution of disodium salt of *N,N'*-bisacryloylcystine was acidified with 1M HCl and extracted several times with 9:1 v:v mixture of dichloromethane

and isopropanol. The combined organic phase was dried with  $\text{MgSO}_4$  and the solvent was evaporated. Nevertheless, the dicarboxylic acid was not stable and therefore was converted quantitatively into the disodium salt in methanol by adding sodium hydroxide. The methanolic solution of disodium salt was added dropwise into diethyl ether, the salt precipitated and the precipitate was filtered and dried under high vacuum.

NMR and mass characterization of the product:  $^1\text{H}$  NMR (200MHz,  $\text{D}_2\text{O}$ )  $\delta$ = 6.50-6.10 (2H, m,  $\text{CH}_2=\text{CH}-\text{CONH}-$ ), 5.90-5.75 (1H, m,  $\text{CH}_2=\text{CH}-\text{CONH}-$ ), 4.70-4.55 (1H, m,  $\text{CH}_\alpha$ ), 3.95-3.20 (1H, m,  $\text{CH}_\beta$ ), 3.10-2.95 (1H, m,  $\text{CH}_\beta$ ).

ESI HR calc. for  $\text{C}_{12}\text{H}_{14}\text{N}_2\text{O}_6\text{S}_2\text{Na}_2$  414.9986 found 414.9971  $[\text{M}+\text{Na}]^+$  (disodium salt of  $N,N'$ -bisacryloylcystine)

ESI HR calc. for  $\text{C}_{12}\text{H}_{15}\text{N}_2\text{O}_6\text{S}_2$  347.0371 found 347.0365  $[\text{M}+\text{H}]^+$  ( $N,N'$ -bisacryloylcystine)

### ***2.3. Synthesis of poly( $N$ -isopropylacrylamide) cross-linked with $N,N'$ -bisacryloylcystine (pNIPA-BISS) microgel***

Microgels were obtained using the surfactant-free emulsion polymerization.<sup>35</sup> NIPA and BISS were dissolved in 195 mL of deionized water in a three-neck flask equipped with a magnetic stirrer (set at 1400 rpm during the entire polymerization), reflux condenser, inlet and outlet of inert gas. The total concentration of NIPA and amino acid derivative was kept constant at 100 mM. The microgels were synthesized with the mole fraction of the amino acid derivative,  $Y_{\text{solution}}$ , equal in the pre-gel solution to 0, 1 and 3 %.

The monomer solution was purged with argon for 0.5 h to remove oxygen and heated up in an oil bath at 70 °C. Then KPS (0.1 g dissolved in 5 mL of deionized and degassed water) was added to initiate the polymerization. The reaction continued for 7 h under an argon blanket. After that the solution was cooled down to room temperature. The schemes of the synthesis and the structure of the obtained microgel polymeric network are shown in Figure 1. Next the microgels were purified by placing them in a dialysis tube with a 10000

Da molecular weight cutoff (Spectra/Por® 7 Dialysis Membrane) and thus removing the oligomers and the unreacted substrates. The microgels were dialyzed against 5 L of water for two weeks at room temperature; water was changed daily. The dialysis was considered complete when conductivity of dialyzate was close to that of pure water (conductivity measurements were carried out using a Radiometer, model CDM230 conductometer). Finally the microgel solution was filtered via a syringe inline glass filter with pore size of 1-2  $\mu\text{m}$ .

#### ***2.4. Determination of amount of N,N'-bisacryloylcystine incorporated into polymeric network of pNIPA-BISS microgels***

The amount of BISS incorporated into the polymer network of the microgels was determined photometrically using Ellman's reagent. A sample of dried microgel was added to sodium borohydride solution. Disulphide crosslinker was reduced to the thiol groups and then the excess of  $\text{NaBH}_4$  was neutralized with HCl. Next excess of Ellman's reagent (DTNB) in phosphate buffer (pH = 8, 0.1 M) was added to the reduced microgels. Absorbance was measured at 412 nm using a Thermo Scientific Evolution 60 UV-Vis spectrophotometer. DTNB reacted with the thiol compound (R-SH, product of the reduction of the disulfide bonds) and formed an adduct with thiol-5-thio-2-nitrobenzoic acid (RS-TNBA). This was followed by release of one equivalent of 5-thio-2-nitrobenzoic acid (TNBA). Since the released TNBA has a strong absorbance at 412 nm in neutral and slightly basic solutions, therefore, UV-VIS spectrophotometric quantification of the released TNBA enables the determination of thiols in the samples. The molar absorptivity (molar extinction coefficient) of TNBA in the buffer system at 412 nm is reported to be  $14\ 150\ \text{M}^{-1}\text{cm}^{-1}$ .<sup>36</sup>

#### ***2.5. Instrumental***

##### *Dynamic Light Scattering*



Hydrodynamic diameter of the dilute aqueous microgel particles dispersions was determined using a Malvern Zetasizer instrument (Nano ZS, UK) fitted with a 4mV He-Ne laser ( $\lambda = 632.8 \text{ nm}$ ) as the light source at the scattering angle of  $173^\circ$ . The solutions of microgel were passed through a 1-2  $\mu\text{m}$  glass-fiber membrane filter just before measurement. The solutions were equilibrated at selected temperatures for 5 min before measurement. The zeta potential was measured using the same instrument. A folded capillary cell with gold electrodes was employed for this purpose. The analyzer calculated the zeta-potential from the electrophoretic mobility using the Henry equation and the Smoluchowski approximation.

The mean molecular weight of polymers that appeared after degradation of the microgels was measured via the static light scattering technique using toluene and water as the standard and solvent, respectively. The microgel solutions of a range of concentration from 0.25 to 1.0  $\text{g L}^{-1}$  were treated with DTT. Four concentrations of each microgel solution were examined and the obtained data were used to construct the Debye plots. The mean molecular weight was obtained from that plot.

#### *Transmission Electron Microscopy (TEM)*

The samples for TEM were prepared by placing a drop of aqueous pNIPA-BISS microgel on a formvar-coated copper grid and allowing them to dry in air. All samples were examined using a Libra 120 microscope (Zeiss).

#### *Scanning Electron Microscopy (SEM)*

The SEM images were taken with a Merlin (Zeiss) microscope at 3 kV. The samples were first dried completely in a hot-air oven at  $50^\circ\text{C}$  and next covered with a thin layer of sputtered Au-Pd alloy to a depth of approximately 3 nm using a Polaron SC7620 Mini Sputter Coater.



## ***2.6. Sample preparation for examination of influence of temperature, pH, ionic strength and reducing agents on properties of pNIPA-BISS microgels***

Dialysis-purified pNIPA-BISS microgels were centrifuged (1400 rpm, 30 min, 10 °C, an Eppendorf Centrifuge model 5430 R with a FA-45-30-11 rotor) and the solution (supernatant) was removed. The pNIPA-BISS gel was then soaked in aqueous solutions of different pH and ionic strength and of reducing agent (either DTT or GSH). pH was changed by adding either HCl or NaOH and was monitored with a pH/ion meter (Mettler Toledo, model SevenGo-SG2). The final pH value was measured just before the measurements. The ionic strength was kept at a constant level (0.01 M) by adding NaCl. Additionally, in all experiments where the reducing agents were used, pH was kept close to 5.0.

## ***2.7. Determination of load and release of DOX***

### *Loading of DOX*

DOX, an anticancer drug, was selected for the investigation of efficiency of drug loading and consecutive controlled release into and from the pNIPA-BISS(3%) microgels, respectively. DOX loading in the microgels was carried out via the incubation method. 1 mL of pNIPA-BISS(3%) microgels (13.50 mg mL<sup>-1</sup>) was centrifuged and dispersed in 1 mL of phosphate buffer solution (pH 7.4). Next, 0.25 mg of DOX was added. The mixed solution was kept overnight at 25°C without stirring to allow DOX to reach the absorption equilibrium in the microgels. The obtained gel dispersion was then centrifuged to collect the DOX-loaded pNIPA-BISS(3%) microgels and after that was washed five times with 1 mL of phosphate buffer solution to remove not adsorbed- and the surface adsorbed DOX. The DOX amount loaded in pNIPA-BISS(3%) microgels was determined by separating the microgels, through centrifugation (14000 rpm min<sup>-1</sup>, 50 min), from the supernatant containing free DOX. and was calculated by subtracting the weight of DOX. Concentration of DOX dissolved was determined spectrophotometrically by measuring absorbance at 480 nm.



### *In vitro drug release*

Efficiency of the release of the drug from pNIPA-BISS(3%) microgels was evaluated by employing the dialysis approach. The DOX-loaded pNIPA-BISS(3%) microgels containing a known amount of DOX were dispersed in 3 mL of either a phosphate buffer of pH 7.4 or in acetate buffer (pH 5.0) and transferred into a dialysis bag (MWCO, 10 kDa). The bags were dialyzed against 20 mL of the corresponding buffer (pH = 7.4 or 5.0) containing 10 mM GSH or without GSH, and gently stirred (300 rpm) at 37°C. The final concentration of microgel was ca. 1 mg ml<sup>-1</sup>. It was assumed that the drug release started as soon as the dialysis bag was placed in the reservoir. The released drug was sampled outside the dialysis bag by using a pump and a flow cell. The concentration of released DOX was determined by measuring the absorbance at 480 nm.

### **2.8. Cell culture**

HT29 human adenocarcinoma colon cell line was obtained from ATCC (American Type Culture Collection) and was tested negatively for mycoplasma using Universal Mycoplasma Detection Kit, ATCC-30-1012K (ATCC). Cells were grown in McCoy's 5A medium (Sigma-Aldrich, St Louis, MO, USA) supplemented with 10% heat-inactivated fetal bovine serum and antibiotics (100 µg/ml streptomycin, 100 U/ml penicillin), in a 5% CO<sub>2</sub> atmosphere at 37°C. Under these growth conditions, the cell-doubling time was 24 h. All experiments were performed with the cells in the exponential phase of growth.

### **2.9. Cytotoxicity assay**

Cell viability was measured by using MTT (3-(4,5-dimethylthiazol-2-yl)-2,5-diphenyltetrazolium bromide, Sigma-Aldrich, St Louis, MO, USA) assay. Briefly, cells (2x10<sup>4</sup>/well) were seeded on 24-well plates and exposed to different concentrations of pNIPA-BISS(3%) microgels, DOX-loaded pNIPA-BISS(3%) microgels and unbound DOX for 72 h. The solutions of these agents were prepared in sterile water. At the end, 0.5 mg/ml

MTT was added to each well and then incubated for 3 h at 37°C. The culture medium was removed and crystals of formazan were dissolved in DMSO. Finally, the absorbance was measured at 540 nm using a microplate reader (iMark™, Bio-Rad, Hercules, CA, USA). The cytotoxic effect of treatment with the drugs was expressed as the IC<sub>50</sub> value (drug concentration required to inhibit cell growth by 50% compared to untreated control cells).

### 3. Results and discussion

Selected SEM and TEM micrographs of microgels containing various amounts of BISS are shown in Figure 2. As it can be seen, all the microgels were rather spherical, including those without BISS cross-linker; however, a careful analysis of the SEM images of pNIPA microgels shows that the spherical shape of the particles was significantly deformed. It can also be concluded that microgel size increases with increasing BISS content. The particles were evenly dispersed, especially in the case of microgels with the highest quantity of disulfide crosslinking. The formation of stable, uncrosslinked microgel particles has been attributed to physical entanglements of the chains during the synthesis.<sup>37</sup>

The amount of BISS incorporated into the polymer network, based on the amount of thiol groups obtained after reduction of the disulfide bonds of BISS, was determined photometrically using Ellman's reagent. The content of the thiol groups in the polymeric network of the microgels was  $196 \mu\text{mole g}^{-1}$  (pNIPA-BISS(1%)) and  $670 \mu\text{mole g}^{-1}$  (pNIPA-BISS(3%)). Basing on these values the amounts of BISS were calculated to be 1.2% and 4.1% for pNIPA-BISS(1%) and pNIPA-BISS(3%), appropriately. The contents of crosslinker in the final gel particles was higher compared to initial substrate mixture probably because proportionally less N-isopropylacrylamide reacted compared to BISS and the unlinked chains were simply dialyzed out after the synthesis. The yields of the synthesis of gel nanoparticles were circa 70% and 80% for pNIPA-BISS (1%) and pNIPA-BISS (3%), respectively. The zeta potential for the obtained microgels was measured and the corresponding data are presented in Figure 3. The observed decrease in zeta potential with increase of BISS is reasonable because the cross-linker introduces negative charge (ionized carboxylic groups) to the network.<sup>38</sup>

The influence of temperature on the swelling behavior of the microgels containing different amounts of amino acid is shown in Figure 4. The temperature dependencies of the

equilibrium swelling ratio for the pNIPA-BISS microgels were constructed using the changes in hydrodynamic diameter of the microgels. The hydrodynamic diameters were determined using the dynamic light scattering method (DLS). Assuming that Brownian motion stood behind the diffusion of the particles, the corresponding diffusion coefficient was obtained from the decay of the autocorrelation function. Then the hydrodynamic diameter ( $D_h$ ) of the microgel particles could be calculated using the Stokes-Einstein equation<sup>35,39</sup>

$$D_h = \frac{kT}{3\pi\eta D} \quad (1)$$

where  $D_h$  - hydrodynamic diameter,  $k$  - Boltzmann constant,  $T$  - temperature,  $\eta$  - solvent viscosity and  $D$  - diffusion coefficient.

By analyzing the swelling behavior of the microgels it can be concluded that an increase in the content of amino acid leads to: 1) a decrease in microgel size at a temperature lower than the volume phase transition temperature (e.g. at 25°C,  $D_h$  equaled 1589, 982 and 943 nm for pNIPA, pNIPA-BISS(1%) and pNIPA-BISS(3%), respectively), and 2) an increase in microgel size at a temperature higher than the volume phase transition temperature (e.g. at 40 °C,  $D_h$  equaled 311, 367 and 436 nm for pNIPA, pNIPA-BISS(1%) and pNIPA-BISS(3%), respectively). This can be explained by the fact that less intensively cross-linked structure can swell more solvent, and that an increase in cross-linker density leads to more packed structures. It is really worth of underlining that the presence/increase of linker leads to limiting of the amount of water absorbed in the gel and makes the net more resistant to the total shrinking after VPTT. Such action of crosslinkers was already reported in the literature.<sup>16,40</sup>

The observed trends in size of shrunken microgels are in agreement with the data obtained by SEM and TEM. Additionally, an increase in the content of amino acid leads to an increase in the volume phase transition temperature (VPTT). It is well known that hydrophilic groups can increase the VPTT, while hydrophobic ones cause the opposite result.<sup>41,42</sup> The unmodified

pNIPA microgel was shown to have a VPTT consistent with the literature value given for the gels based on *N*-isopropylacrylamide, i.e. circa 32 °C.<sup>43</sup>

Next, we investigated the influence of the ionic strength on the swelling behavior of pNIPA-BISS microgels. The temperature dependencies of the swelling ratio were examined for several selected values of salt concentration; they are presented in Figure 5. The microgel without BISS became unstable and gelled / agglomerated as temperature increased; this took place already at such small ionic strength as 0.01 M (see photo in left part of Figure 5). The temperature, at which the microgels started to be unstable, decreased as the salt concentration was increased. The pNIPA-BISS(1%) microgel dispersion was stable when concentration of NaCl was lower than 0.1 M. At circa 0.1 M the microgel dispersion became unstable and flocculated as temperature increased. For 0.2 M NaCl the aggregation could be observed with a naked eye (see photo in central part of Figure 5). A very good stability vs. salt concentration was exhibited by the pNIPA-BISS(3%) microgel. At the higher salt concentrations (0.8 and 1.5 M) the microgels lost their typical temperature sensitivity and were shrunken at the entire temperature range. Generally, the microgels flocculated in the shrunken state when concentration of the electrolyte was sufficiently high and the electrostatic repulsions between them were weakened.<sup>18</sup> An increase in salt concentration caused a decrease in volume-phase-transition temperature that led to flocculation of the samples at lower temperatures. The microgels became more resistant to the flocculation process when they contained more ionized groups and were stronger charged. An increase in content of BISS caused an increase in content of negatively charged carboxylic groups and changed correspondingly the zeta potential (see data in Figure 3). So, the presence of BISS in the polymeric networks of the investigated microgels gave them better stability in the presence of the salt.

Influence of pH on the swelling behavior and stability of the microgels was also investigated. The temperature dependencies of the swelling ratio were examined for selected values of pH

and are presented in Figure 6. Ionic strength was kept constant at a 0.01 M level by adding appropriate amount of NaCl to the solution. At alkaline pH the microgels exhibited a bigger diameter before and after phase transition. Under such conditions almost all carboxylic groups are ionized and the microgels were swollen due to the electrostatic repulsions and an increase in the osmotic pressure between the solution and the gel. When pH decreased and solution became weakly acidic the diameter of microgels decreased before and after volume phase transition. This is apparently related to the protonation of a part of the carboxylic groups. Further acidification of the solution resulted in a behavior similar to that seen for the higher ionic strength. Due to the protonation of the carboxylic groups and the corresponding drop in the negative charge the microgels became unstable and aggregated when temperature went up, especially when temperature increased above the cloud-point/volume-phase-transition temperature.<sup>18</sup> The microgels with smaller surface charges had a tendency to aggregate under less acidic condition than the gels with bigger surface charges. pNIPA-BISS(1%) microgels flocculated already at pH ca. 4 while pNIPA-BISS(3%) became unstable and aggregated at pH of ca. 3.

We have also done some experiments with pNIPA in different pH (2.7 – 11.6) and constant ionic strength (0.01 M NaCl). In all cases, at temperatures over 33°C pNIPA loses stability and aggregates. The size of gel microparticles, below phase-transition temperature, was practically independent of pH.

Next, we investigated the influence of the type of the reducing agent (DTT and GSH were employed) on the degradation of the microgels cross-linked with the derivative of cystine. Samples of the microgels were treated with 0.01 M solution of DTT and GSH. The results were examined with SEM and TEM. The images obtained by both techniques revealed substantial changes in microgel morphology. In Figure 7B, selected SEM images of degraded microgels are shown. As it can be seen the spherical structure of the microgel particles was



completely damaged. Selected TEM images (see Figure 7A) show that the microgels degraded into smaller fragments after 1-day treatment. While the pNIPA-BISS(1%) microgels almost completely degraded the pNIPA-BISS(3%) degraded only incompletely after one-week reaction with the reducing agent. This can be explained by the fact that during microgel synthesis some unwanted side reactions may take place. The disulfide bond may be homolytically cleaved at high temperatures what results in sulfur radical formation. Radical attack may lead to the formation of the thioether which is not susceptible to the reduction process and strengthens the net.<sup>44</sup>

The mean molecular weights of the degraded microgels have been estimated using the Debye plot of scattering intensity vs. microgel concentration. The results were the following:  $3.15 \times 10^5$  and  $7.2 \times 10^6$  Da, for pNIPA-BISS(1%) and pNIPA-BISS(3%), respectively.

To evaluate the usefulness of the microgel cross-linked with the cystine derivative as a drug carrier we selected pNIPA-BISS(3%) microgels and DOX as a model anti-cancer drug. This selection was done since pNIPA-BISS(1%) microgels flocculated under the release conditions. Drug loading capacity ( $n_{\text{DOX}}/n_{\text{BISS}} \cdot 100\%$ ) was bigger than 10% vs. the amount of cross-linker. In Figure 8 the influence of pH and the presence of GSH on release profiles of DOX at 37 °C is shown. It can be seen that DOX cumulative release equaled circa 40% at pH 7.4 after 2 h. Under acidic conditions (pH 5.0) an increase in cumulative release to ca. 50% was observed. However, the highest increase in cumulative release, to ca. 80%, was noted at pH 5.0 and in the presence of GSH. So, a departure of environmental conditions from those corresponding to the blood medium (pH~7.4) to those characteristic for the affected cells (pH~5.0 and  $C_{\text{GSH}} \sim 10$  mM) should trigger a release of a significant amount of loaded DOX.

Cytotoxicity of pNIPA-BISS(3%) microgels, DOX-loaded pNIPA-BISS(3%) microgels and free DOX was studied against human colon carcinoma HT29 cells. This cell line was selected because it is representative of solid tumors which are very often resistant to antitumor therapy

and the colon cancer is one of the most common types of cancer in the world. MTT proliferation assay revealed that after 72-h exposure to DOX-loaded pNIPA-BISS(3%) microgels and DOX alone, the viability of HT29 cells decreased in a dose-dependent manner, see Figure 9. Interestingly, DOX-loaded pNIPA-BISS(3%) microgels exhibited comparable cytotoxicity to free Doxorubicin ( $IC_{50} = 0.81$  and  $0.75 \mu\text{M}$ , for DOX-loaded pNIPA-BISS(3%) microgels and DOX alone, respectively). It should be added that the pNIPA-BISS(3%) microgels without DOX did not inhibit proliferation of HT29 cells in a wide range of concentration, including doses equivalent to  $IC_{50}$  of DOX-loaded pNIPA-BISS(3%) microgels, see inset in Figure 9. The relative standard deviation of the cytotoxicity measurements did not exceed 8%.

#### 4. Conclusions

The obtained results indicate that the diacryloyl derivative of cystine can be incorporated into the thermoresponsive microgels by surfactant free emulsion polymerization. The synthesized microgels formed spherical particles; their size distribution was satisfactorily narrow. The derivative of cystine was the cross-linker and made the microgels degradable and sensitive to pH. An increase in content of the diacryloyl derivative of cystine led to an increase in both: temperature of volume phase transition and stability of the obtained microgels. It was found that the microgels with 3% content of the cystine derivative were highly stable in a wide range of temperature, pH and ionic strength and that included the physiological conditions (pH 7.4, 0.15 M, 37 °C). We found that the reduction-induced degradation of the obtained microgels, by a 0.01 M solution of dithiothreitol or glutathione, led to the degradation of the microgels. Additionally, the presence of the carboxylic group in the cross-linker allowed the load of doxorubicin into the microgels and then the efficient release of the drug under conditions similar to those in the affected (by cancer) cells (pH~5.0 and  $C_{\text{GSH}} \sim 10 \text{ mM}$ ). The DOX loaded microgels were cytotoxic against selected cancer HT29 cells similarly do DOX

alone, while unloaded gel microparticles did not inhibit proliferation of the cells. These properties make the microgels cross-linked with the derivative of cystine interesting as useful carriers in directed drug delivery systems.

### **Acknowledgment**

This work was supported by Iuventus Grant no. IP2012 015272 from the Polish Ministry of Science and Higher Education and by Grant no. 2011/01/D/ST5/05866 from the National Science Center of Poland.

## Figure legends

### Figure 1.

Scheme of synthesis and structure of microgel based on *N*-isopropylacrylamide cross-linked with *N,N'*-bisacryloylcystine.

### Figure 2.

SEM (A) and TEM (B) images of microgels with various amount of BISS.

### Figure 3.

Zeta potential ( $\zeta$ ) measured for microgels with various amount of BISS.

### Figure 4.

Change in hydrodynamic diameter of microgels with various amount of BISS as function of temperature.

### Figure 5.

Hydrodynamic diameter plotted vs. temperature for microgels dispersed in solutions of different salt (NaCl) concentration and for microgels with various amount of BISS. Insets show gelled pNIPA and flocculated pNIPA-BISS(1%) due to high concentration of salt, and stable colloidal solution of pNIPA-BISS(3%).

### Figure 6.

Hydrodynamic diameter as function of temperature and pH for pNIPA-BISS(1%) and pNIPA-BISS(3%) microgels

### Figure 7.

TEM (A) and SEM (B) images of the products of degradation of microgels cross-linked with 1% and 3% of BISS by DTT and GSH

### Figure 8.

DOX release profiles from DOX-loaded pNIPA-BISS(3%) microgels for different pH and presence of GSH, T=37°C.

## Figure 9

Cytotoxicity of DOX-loaded pNIPA-BISS(3%) microgels and free DOX against human colon carcinoma HT29 cells after 72 h of treatment, assessed by MTT assay. Growth inhibition is expressed as percentage of control value (untreated cells). Inset: Cytotoxicity of DOX-free pNIPA-BISS(3%) microgels against HT29 cells under identical experimental conditions.

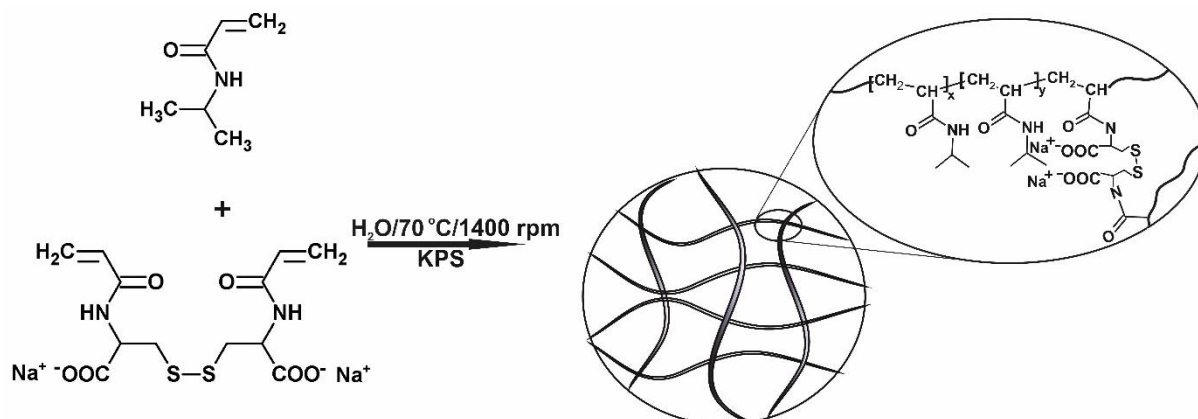


Figure 1

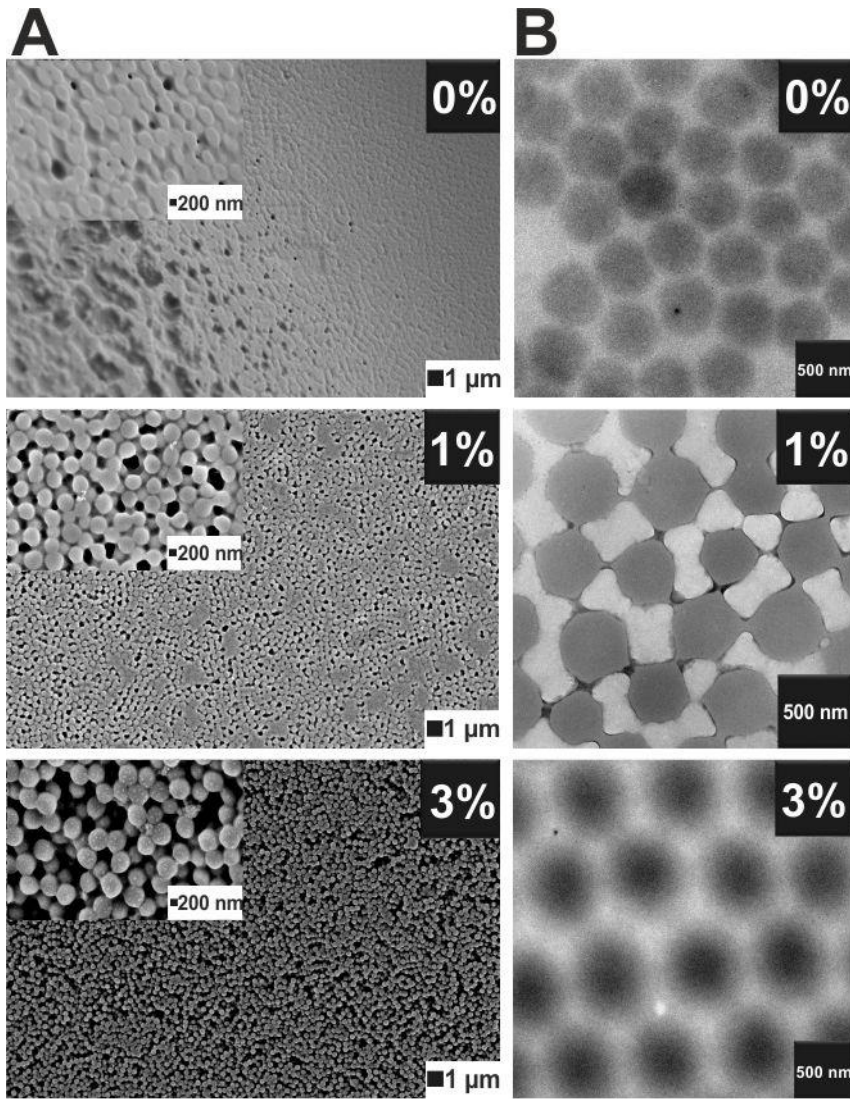


Figure 2

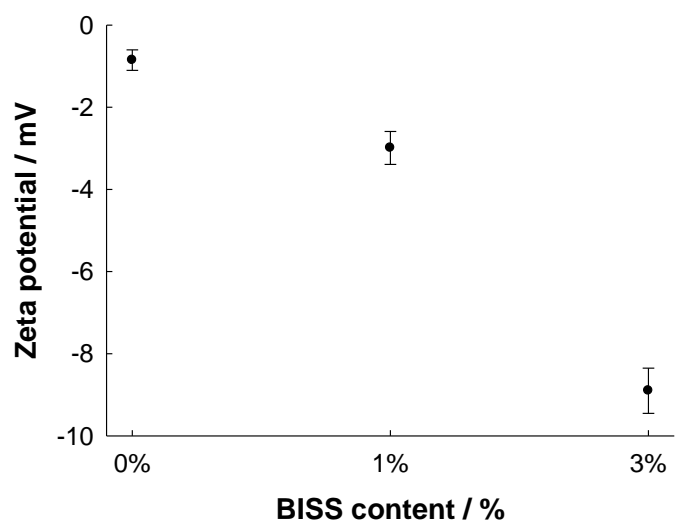


Figure 3



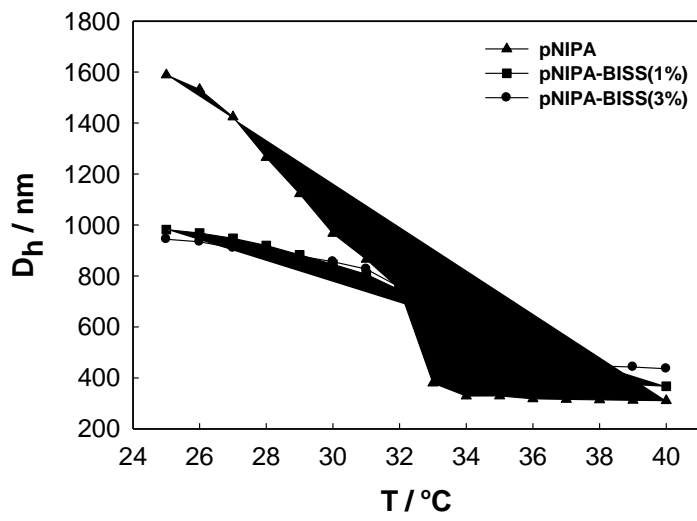


Figure 4

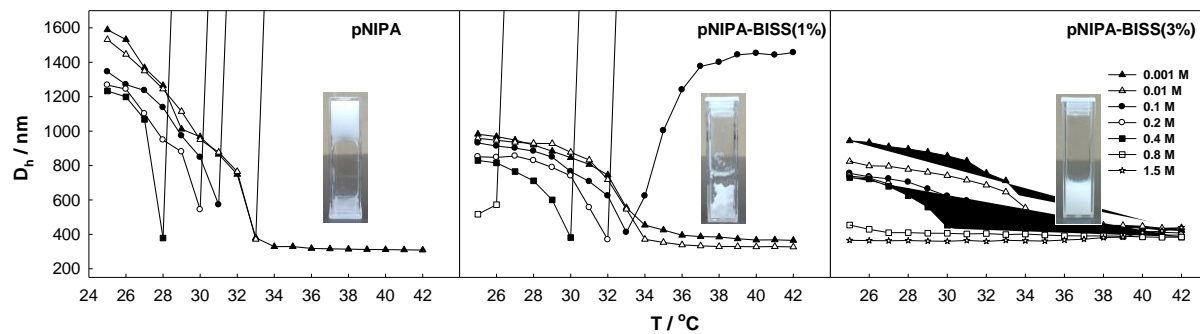


Figure 5

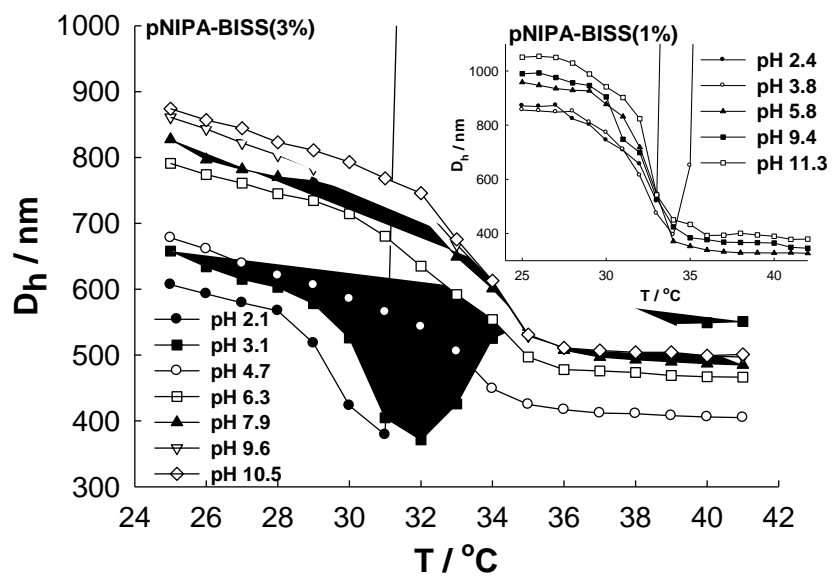


Figure 6

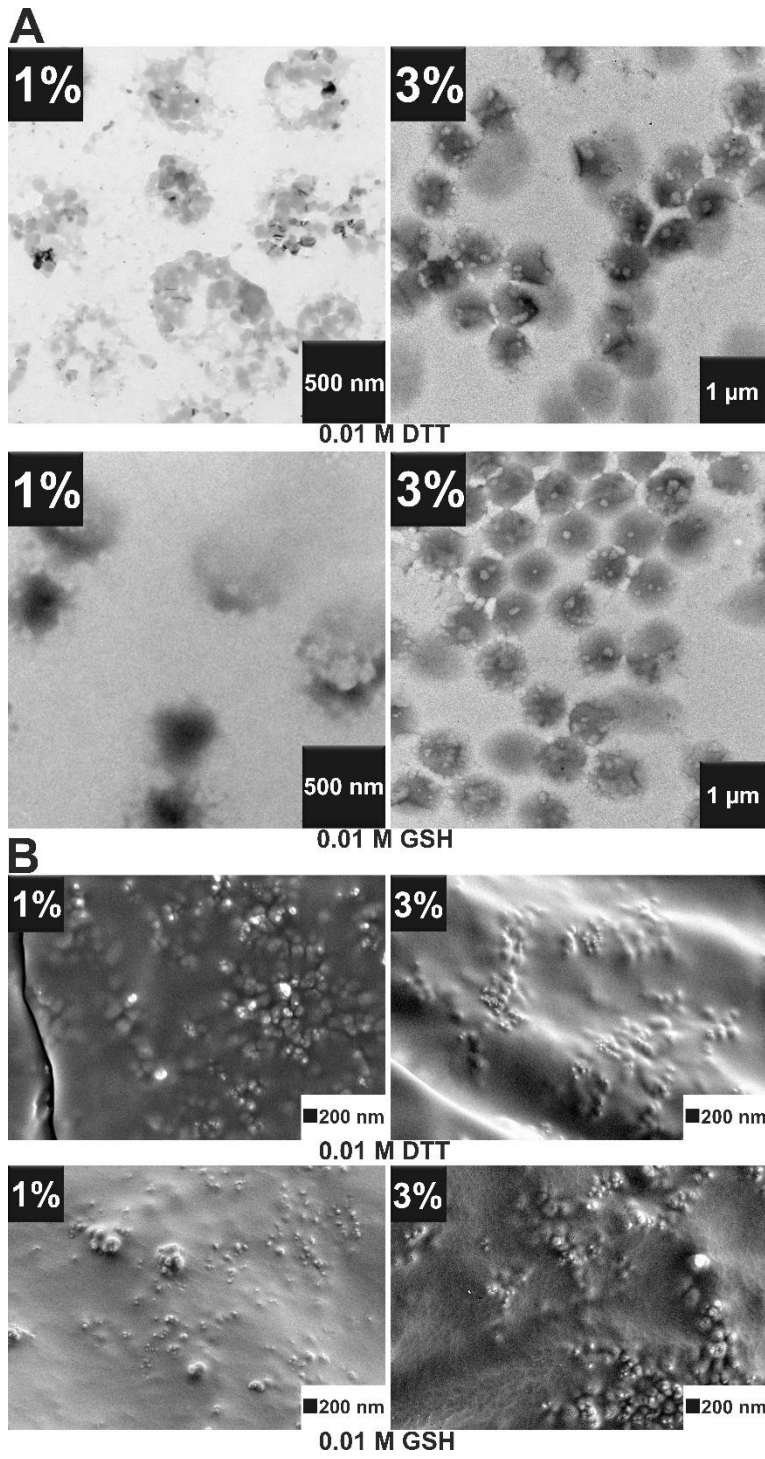


Figure 7

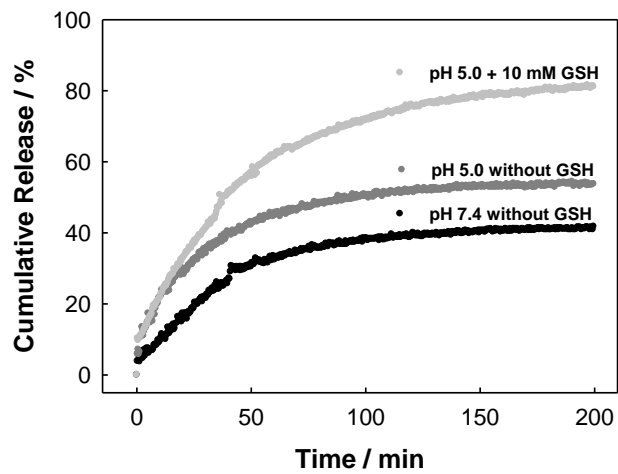


Figure 8

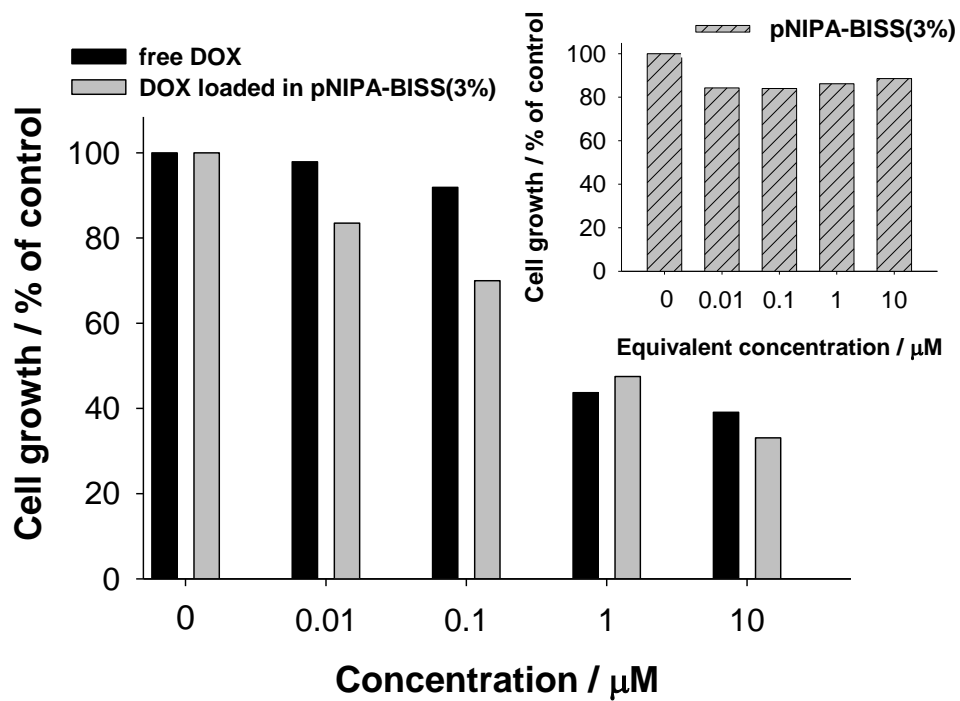


Figure 9

## References

- 1 T. Ngai, S. H. Chen, H. Auweter, *Chem. Commun.*, 2005, 331.
- 2 T. Lane, J. L. Holloway, A. H. Milani, J. M. Saunders, A. J. Freemont, B. R. Saunders, *Soft Matter*, 2013, **9**, 7934.
- 3 R. Turcu, V. Socoliuc, I. Craciunescu, A. Petran, A. Paulus, M. Franzreb, E. Vasile, L. Vekas, *Soft Matter*, 2015, **11**, 1008.
- 4 M. Maćkiewicz, J. Romański, M. Karbarz, *RSC Adv.*, 2014, **4**, 48905.
- 5 X. Zhang, C. Gao, S. Lu, H. Duan, N. Jing, D. Dong, C. Shi, M. Liu, *J. Mater. Chem. B*, 2014, **2**, 5452.
- 6 M. Maćkiewicz, T. Rapecki, Z. Stojek, M. Karbarz, *J. Mater. Chem. B*, 2014, **2**, 1483.
- 7 C. Schunicht, A. Biffis, G. Wulff, *Tetrahedron*, 2000, **56**, 1693.
- 8 M. A. Willard, L. K. Kurihara, E. E. Carpenter, *Int. Mater. Rev.*, 2004, **49**, 125.
- 9 M. Varma, A. Kaushal, S. Garg, *J. Controlled Release*, 2005, **103**, 499.
- 10 J. C. Gaulding, A. B. South, L. A. Lyon, *Colloid Polym. Sci.*, 2013, **291**, 99.
- 11 J. K. Oh, R. Drumright, D. J. Siegwart, K. Matyjaszewski, *Prog. Polym. Sci.*, 2008, **33**, 448.
- 12 G. M. Eichenbaum, P. F. Kiser, A. V. Dobrynin, S. A. Simon, D. Needham *Macromolecules*, 1999, **32**, 4867.
- 13 H. Malonne, F. Eeckman, D. Fontanie, A. Otto, L. D. Vos, A. Moes, J. Fontaine, K. Amighin, *Eur. J. Pharm. Biopharm.* 2005, **61**, 188.
- 14 G. H. Hsiue, S. H. Hsu, C. C. Yang, S. H. Lee, I. K. Yang, *Biomaterials*, 2002, **23**, 457.
- 15 H. Vihola, A. Laukkanen, L. Valtola, H. Tenhu, J. Hirvonen, *Biomaterials*, 2005, **26**, 3055.
- 16 J. C. Gaulding, M. H. Smith, J. S. Hyatt, A. Fernandez-Nieves, L. A. Lyon, *Macromolecules* 2012, **45**, 39.
- 17 Y. J. Pan, Y. Y. Chen, D. R. Wang, Ch. Wei, J. Guo, D. R. Lu, C. C. Chu, C. C. Wang, *Biomaterials*, 2012, **33**, 6570.
- 18 X. Zhang, S. Lü, C. Gao, C. Chen, X. Zhang, M. Liu, *Nanoscale*, 2013, **5**, 6498.
- 19 Y. Zhan, M. Gonçalves, P. Yi, D. Capelo, Y. Zhang, J. Rodrigues, C. Liu, H. Toma's, Y. Li, P. He, *J. Mater. Chem. B*, 2015, DOI: 10.1039/c5tb00468c.
- 20 E. Emilriti, E. Ranucci, P. Ferruti, *J. Polym. Sci., Part A: Polym. Chem.*, 2005, **43**, 1404.
- 21 T. Yuan, Y. Wang, W. Cao, Y. Sun, J. Liang, Y. Fan, X. Zhang, *J. Bioact. Compat. Polym.*, 2014, **29(5)**, 458.
- 22 K. Kaniewska, J. Romanski, M. Karbarz, *RSC Adv.*, 2013, **3**, 23816.
- 23 G. Wu, Y. Z. Fang, S. Yang, J. R. Lupton, N. D. Turner, *J. Nutr.*, 2004, **134**, 489.
- 24 F. S. Du, Y. Wang, R. Zhang, Z. C. Li, *Soft Matter*, 2010, **6**, 835.
- 25 F. H. Meng, W. E. Hennink, Z. Zhong, *Biomaterials*, 2009, **30**, 2180.
- 26 S. Bauhuber, C. Hozsa, M. Breunig, A. Gopferich, *Adv. Mater.*, 2009, **21**, 3286.
- 27 G. Saito, J. A. Swanson, K. D. Lee, *Adv. Drug Delivery Rev.*, 2003, **55**, 199.
- 28 F. Meng, W. E. Hennink, Z. Zhong, *Biomaterials*, 2009, **30**, 2180.
- 29 P. Kuppasamy, M. Afeworki, R. A. Shankar, D. Coffin, M. C. Krishna, S. M. Hahn, *Cancer Res.*, 1998, **58(7)**, 1562.
- 30 J. Ding, J. Chen, D. Li, C. Xiao, J. Zhang, C. He, X. Zhuang, X. Chen, *J. Mater. Chem. B*, 2013, **1**, 69.
- 31 J. Yue, R. Wang, S. Liu, S. Wu, Z. Xie, Y. Huang, X. Jing, *Soft Matter*, 2012, **8**, 7426.
- 32 L. J. Huo, M. Wang, J. Zhou, J. Mohammad, J. M. Zhang, Y. Zhu, Q. Waddad, A. Y. Zhang, *Biomaterials*, 2012, **33**, 2310.
- 33 H. Wei, R. X. Zhuo, X. Z. Zhang, *Prog. Polym. Sci.*, 2013, **38**, 503.
- 34 Pat., WO2005/27873 A2, 2005.

- 35 I. Galaev, B. Mattiasson, *Smart Polymers, Applications in Biotechnology and Biomedicine*, CRC Press, New York, 2nd ed., 2008.
- 36 P. W. Riddles, R. L. Blakeley, B. Zerner, *Meth. Enzymol*, 1983, **91**, 49.
- 37 Y. Chen, S. Sajjadi, *J. Appl. Polym. Sci.*, 2014, **131**, 40781.
- 38 R. A. Bader, A. L. Silvers, N. Zhang, *Biomacromolecules*, 2011, **12**, 314.
- 39 T. Hoare, R. Pelton, *Polymer*, 2005, **46**, 1139.
- 40 I. Varga, T. Gilanyi, R. Meszaros, G. Filipcsei, M. Zrinyi, *J. Phys. Chem. B*, 2001, **105**, 9071.
- 41 G. Liu, X. Li, S. Xiong, L. Li, P. K. Chu, S. Wu, Z. Xu, *J. Fluorine Chem.*, 2012, **135**, 75.
- 42 R. L. Bartlett II, M. R. Medow, A. Panitch, B. Seal, *Biomacromolecules*, 2012, **13**, 1204.
- 43 D. Gan, L. A. Lyon, *J. Am. Chem. Soc.*, 2001, **123**, 7511.
- 44 J. L. Kice, A. Senning, M. Dekker, *Sulfur in Organic and Inorganic Chemistry*, New York, 1971.